

STUDY OF STABILITY OF VARIANTS OF OVINE PRIONS WITH DIFFERENT SUSCEPTIBILITIES TO SCRAPIE

H. Rezaei¹, Y. Choiset², P. Debey³, J. Grosclaude¹ and T. Haertlé^{2}*

¹Virologie et Immunologie Moléculaires (VIM), INRA, F-78352 Jouy-en-Josas, France

²Laboratoire d'Étude des Interactions des Molécules Alimentaires (LEIMA), INRA, F-44316 Nantes, France

³Institut National de la Recherche Agronomique (INRA) UC 806/EA 2703 Muséum National d'Histoire Naturelle, Institut de Biologie Physico-Chimique, 13, rue P. et M. Curie, F-75005 Paris, France

Abstract

Well-defined set of sheep PrP polymorphisms at positions 136, 154 and 171 define susceptibility to scrapie, ranging from very high susceptibility observed for V136-R154-Q171 (VRQ) variant to resistance for A136-R154-R171 (ARR).

To gain insight into the mechanisms of scrapie susceptibility/resistance, the unfolding pathways of the sheep prion protein variants were analysed by differential scanning calorimetry over a wide range of pH. Thermal unfolding occurs, in the 5.0 to 6.0 pH range, through a reversible one-step process while at pH < 4.5 and > 6.0 unfolding intermediates are formed, which are stable in the 65–80°C range. The observed differences correlate with ovine susceptibility to scrapie.

Keywords: scrapie susceptibility/resistance, prion, amyloids, DSC

Introduction

Many hypotheses have been advanced concerning the nature of the infectious agents causing spongiform encephalopathies – or ‘prion diseases’ – but the most widely accepted, the ‘protein only’ hypothesis, proposes a proteic nature of the infectious agent [1, 2]. According to this hypothesis, the main event in the pathogenesis is the conversion of the cellular form of the prion protein (PrP_c) of the host, into a pathogenic isoform (PrP_{sc}) characterized by its insolubility, its high β-sheet content, and its protease resistance. The difference between PrP_{sc} and PrP_c is only conformational because no covalent modifications differentiate PrP_{sc} from PrP_c [3].

In sheep a set of PrP polymorphisms at positions 136, 154 and 171 (sheep numbering) was reported to be connected to scrapie susceptibility [4–7]. The homozygous genotype A136-R154-R171 (ARR) induces a resistant phenotype, when V136-R154-Q171

* Author for correspondence: E-mail: haertle@nantes.inra.fr

(VRQ) confers high scrapie susceptibility phenotype. Between these two extreme variants others were also described, A136-R154-Q171 (ARQ) and (A136-H154-Q171 (AHQ), which are associated with medium and low susceptibility to scrapie, respectively. Although many PrP polymorphisms are reported to influence either the susceptibility of humans and mice to transmissible spongiform encephalopathies (TSE) or the rate of its incubation, no particular genotype is known to completely protect against the pathogenic agent. So far, sheep is the only mammalian species presenting a strong correlation between genotype and susceptibility phenotype.

According to the 'protein only theory', the effect of PrP polymorphisms on the pathogenic transconformation can be explained if these polymorphisms affect the folding pathways or the interactions of the protein with, still ill-defined, factors involved in the PrPc→PrPsc transition. Previous physico-chemical studies concerning the folding energy of different human polymorphic PrPs related to familial TSE did not show any clear-cut differences between them [8, 9]. Previous studies of heat and chemical unfolding of sheep VRQ, ARQ and ARR PrP variants indicated significant differences in their denaturation free energy and in their tertiary structure as revealed by protease finger-printing [10].

To obtain greater insight into the molecular mechanisms of scrapie susceptibility and resistance, the effect of each sheep prion polymorphism on the unfolding pathway was investigated by differential scanning calorimetry over a wide range of pH. It was observed that i) sheep PrP variants form unfolding amyloidogenic intermediates at pH<4.5 and >6.0 in the absence of any chemical treatment and ii) depending on the variant, these intermediates exhibit different behaviour.

Materials and methods

Protein production

All prion variants were purified according to the protocol described previously [10]. The genes encoding the full-length variants (23-234) were cloned in pET 22b+ and expressed by IPTG induction in BL21 DE3 *E. coli*. The expressed prion proteins accumulated in inclusion bodies. After lysis, sonication and solubilization of the inclusion bodies by urea, the purification and renaturation of the prion protein were performed on a Ni Sepharose column by heterogeneous phase renaturation [10], using the intrinsic high affinity of the PrP N-terminal part for metal cations.

After purification, PrP variants were recovered in different buffers covering the 3.0 to 7.2 pH range by G25 Hiprep 26/10 desalting column (Pharmacia) using Akta FPLC chromatography equipment (Pharmacia). The choice of the buffers was based on their low pH variation as a function of temperature: sodium citrate (10 mM) for pH 3.0 and 4.0, sodium acetate (20 mM) for pH 4.5 and 5.0, MES (20 mM) for pH 6.0 and 6.5, MOPS (20 mM) for pH 7.2. Final protein concentration was measured by optical density at 280 nm and assuming an extinction coefficient of 58718.0 M⁻¹ cm⁻¹ deduced from the composition of the protein.

Differential scanning calorimetry (DSC)

Differential scanning calorimetry was performed on a differential scanning calorimetry instrument (VP1-MicroCal). All the experiments were performed at 45 μM protein concentration in a 500 μL cell. An external pressure of 34 psi was applied to the solution and, except in the case of irreversible transitions (see below), the scan rate was 60°C h^{-1} . In the case of reversible folding/unfolding processes (pH 4.5 and 5.0) the calorimetric heat capacity (C_p) vs. temperature were analysed by a two-state transition model using DSC-Origin 5.0 software and the thermodynamic parameters were determined according to the equation

$$C_p(T) = C_{pN} + \left[\frac{K(T)\Delta C_p}{1+K(T)} + \frac{K(T)\Delta H_{\text{vH}}\Delta H_{\text{cal}}}{(1+K(T))^2 RT^2} \right]$$

where $C_p(T)$ is the variation of heat capacity as a function of temperature (T), C_{pN} the heat capacity before transition, $K(T)$ the ratio between the unfolded and the native state, ΔC_p the difference in heat capacity between the folded and unfolded state, ΔH_{vH} and ΔH_{cal} van't Hoff enthalpy and calorimetric enthalpy, respectively.

In the case of irreversible transitions, a theoretical analysis of the DSC curves using the Lumry–Eyring model was applied [12, 13]. This model requires the recording of curves at different scan rates. At a defined temperature scan rate (ν), the half melting temperature (T_m) is linked to the activation energy (E^\ddagger) and the transition probability factor (A) by the relation:

$$\ln(\nu/T_m) = \ln(A R/E^\ddagger) - E^\ddagger/RT_m$$

where R is $8.32 \text{ J mol}^{-1} \text{ K}^{-1}$ and A represents the transmission factor. The first order kinetic rate was determined according to the Arrhenius relation:

$$k = A e^{-E^\ddagger/RT}$$

Assuming that the transition is monomolecular, the activation enthalpy (ΔH^\ddagger) and entropy (ΔS^\ddagger) were determined according to the Eyring theory of the transition state:

$$\Delta H^\ddagger = E^\ddagger - RT$$

$$\ln(A) = -2 + \ln(k_B T/h) + \Delta S^\ddagger/R$$

where k_B is the Boltzman constant, T temperature in K, and h is the Planck constant.

Results

Between pH 4.5 and pH 5.0 (Fig. 2)

At pH 4.5, the DSC curves obtained for all variants show a single endothermic peak characteristic of protein denaturation (Fig. 1a) [14]. The DSC curves are fully reversible as seen for ARQ in Fig. 1c. Values of the van't Hoff (ΔH_{vH}) and calorimetric enthalpy (ΔH_{cal}) calculated from the curves are given in Table 1. As can be seen in Ta-

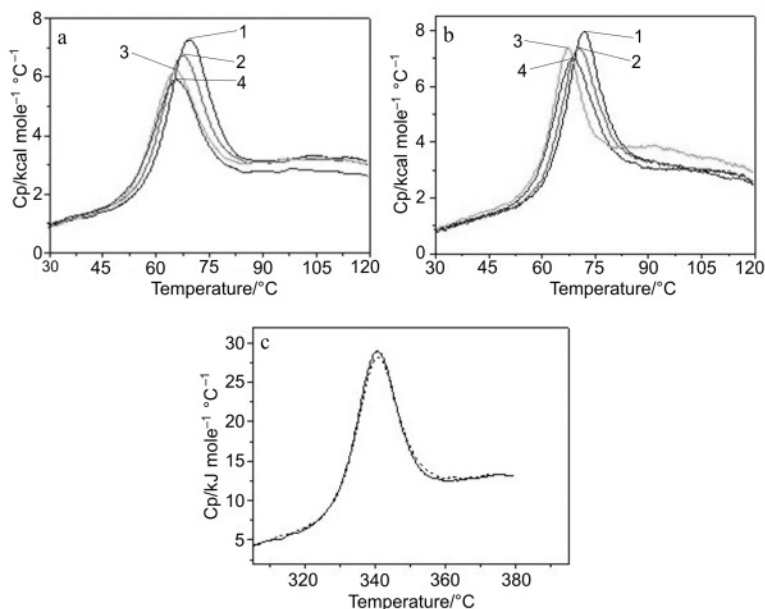


Fig. 1 The DSC curves of unfolding of the different sheep PrP variants at a – pH 4.5 and b – 5.0, and c – reversibility of the denaturation process. In (a) and (b) VRQ is in – 1, ARQ in – 2, AHQ in – 3 and ARR in – 4. (c) The DSC curves obtained for ARQ at pH 4.5 after first heating to 100°C (—) and after one round of heating to 110°C and cooling to 20°C (---)

ble 1, the $\Delta H_{vH}/\Delta H_{cal}$ ratio is close to 1 suggesting for all PrP variants, a two-step denaturation pathway. Similar two-state reversible denaturation process is observed at pH 5.0 for ARR, ARQ and VRQ PrP variants (Fig. 1b), with a similar value of the $\Delta H_{vH}/\Delta H_{cal}$ ratio (Table 1). However, at the same pH, AHQ curves are complex with the emergence of a second denaturation peak, and the $\Delta H_{vH}/\Delta H_{cal}$ ratio >1 suggests a non-two-state model of unfolding (Fig. 1b and Table 1). In addition, analysis of the ΔH_{cal} and ΔG values under conditions of reversible denaturation, i.e. pH 4.5 and 5.0 for all variants except for AHQ at pH 5.0, indicates clearly that at both pHs, variants associated with ovine susceptibility to scrapie are more stable than variants associated with scrapie resistance. This agrees with previous data derived from guanidine-induced denaturation curves [10].

pH < 4.5

According to the DSC curves carried out at pH 3.0 and pH 4.0 (Figs 2a and b), all studied PrP variants exhibit two transitions: the first occurring around 45°C and the second around 110°C at pH 4.0. These types of curves can be explained by the existence of at least one intermediate (*I*) in the denaturation process, stable over a rather wide temperature range (72 to 82°C). In all variants, both transitions are shifted towards lower temperatures at pH 3.0, implying an acidic destabilisation of both folded and intermediate states

Table 1 Thermodynamic parameters of sheep PrP protein unfolding at pH 4.5 and 5.0 for different variants

	pH 4.5				pH 5.0			
	VRQ	ARQ	AHQ	ARR	VRQ	ARQ	AHQ	ARR
	$T_m/^\circ\text{C}$	68.9	67.4	65.3	65.2	71.3	70.1	66.3
$\Delta_{\text{cal}}H/\text{kJ mol}^{-1}$	288.8	262.5	211.5	228.6	249.5	242.0	153.8	230.0
$\Delta_{\text{vH}}H/\text{kJ mol}^{-1}$	272.1	257.1	263.0	243.2	318.9	295.1	396.7	284.2
$\Delta_{\text{vH}}H/\Delta H_{\text{cal}}$	0.9	1.0	1.3	1.1	1.3	1.2	2.6	1.2
$T\Delta S/\text{kJ mol}^{-1}$	250.5	230.0	185.0	202.7	214.7	211.7	134.2	200.0
$\Delta C_p/\text{kJ mol}^{-1} \text{K}^{-1}$	3.07	0.59	0.58	1.1	5.0	4.7	–	4.3
$\Delta G_u^0/\text{kJ mol}^{-1}$	40.1	35.5	28.0	29.7	36.8	34.9	–	32.3

T_m is the temperature of mid-transition, $\Delta_{\text{cal}}H$ the calorimetric enthalpy, $\Delta_{\text{vH}}H$ the van't Hoff enthalpy, ΔG^0 the standard free energy of unfolding, and ΔC_p the heat capacity change between the native and unfolded state

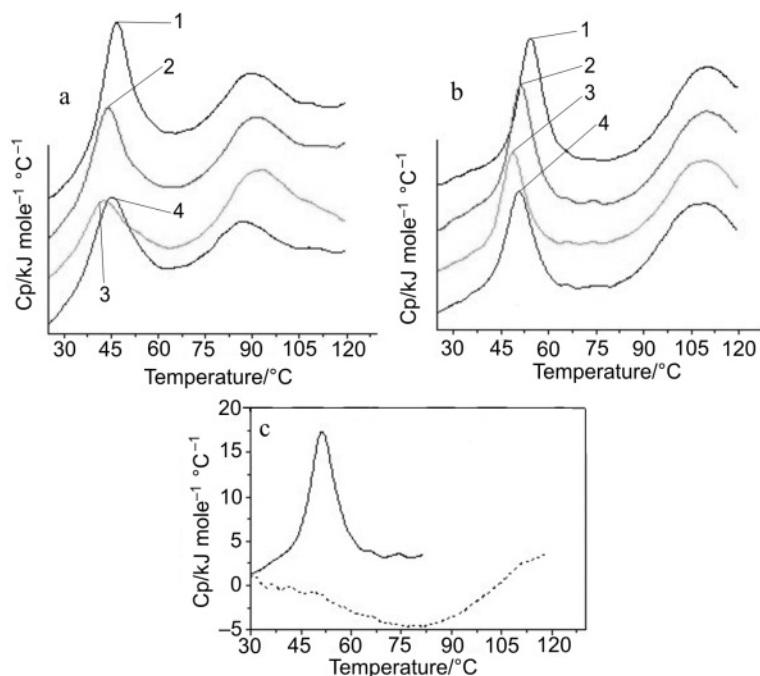


Fig. 2 The DSC curves of unfolding of the different sheep PrP variants at a – pH 3.0 and b – 4.0 and c – irreversibility of the denaturation process. In (a) and (b) VRQ is represented by – 1, ARQ by – 2, AHQ by – 3 and ARR by – 4 lines. (c) The DSC curves obtained for ARQ at pH 4.0 after first heating to 85°C (—) and after one round of heating to 85°C and cooling to 15°C before the second temperature rise (---)

by protonation (Fig. 2a). After one round of heating to 85°C and cooling to 15°C, the second curve shows no variation in the heat capacity, i.e. no thermal transition (Fig. 2c). This demonstrates that the first transition is completely irreversible.

pH > 6.0

At pH 6.0 the curves obtained for ARR, ARQ and VRQ PrP variants show the appearance of another denaturation peak (Fig. 3a), while the magnitude of the second peak in the AHQ curve increases if compared to pH 5.0. The denaturation is irreversible in the case of all PrP variants. Additionally, aggregates are formed after cooling to 20°C (not shown). At higher pH (6.5 and 7.2) and for all variants, the proportion of unfolding intermediate becomes more important (Figs 3b and c) and the aggregation after cooling is observed under all conditions (not shown). At pH 4.0, the first transition disappears completely after one cycle of heating to 85°C and cooling to 15°C (Fig. 3d).

The formation of amyloid fibrils was confirmed by electron microscopy of refolded forms of VRQ and ARR prepared 24 h before at pH 4.0 and 7.2. The images obtained show numerous well structured fibrils of variable length and diameter, the largest being

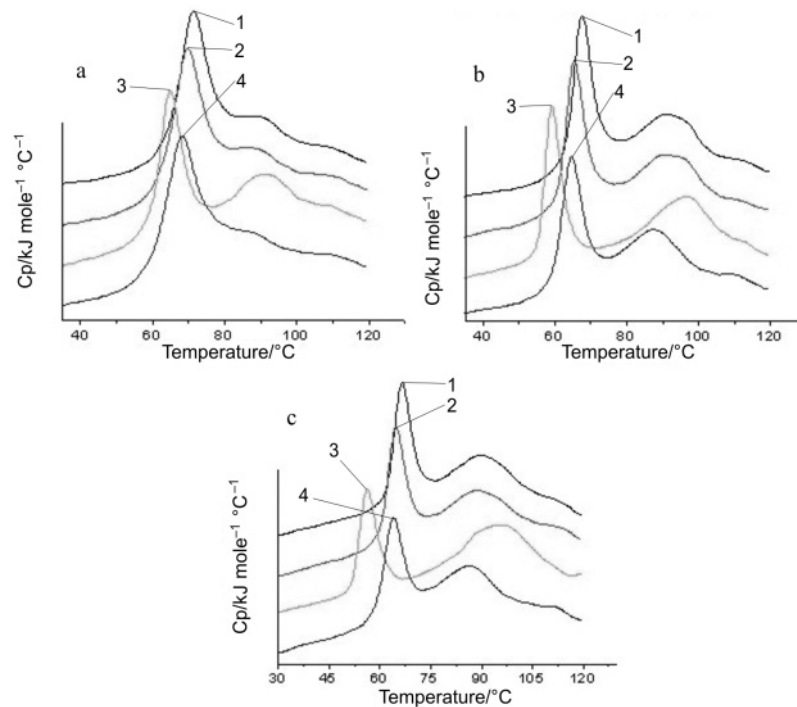


Fig. 3 The DSC curves of unfolding of the different sheep PrP variants at a – pH 6.0, b – 6.5 and c – 7.2 and d – irreversibility of the denaturation process. In (a) and (b) VRQ is represented by – 1, ARQ by – 2, AHQ by – 3 and ARR by – 4 lines. (d) The curves obtained for ARQ at pH 7.2 after first heating to 85°C (—) and after one round of heating to 85°C and cooling to 15°C before the second temperature rise (---)

clearly composed from the lateral association of several individual filaments about 8 nm in diameter (data not shown). There is no qualitative difference between the fibrils obtained from these two variants. The native prion protein used as a control, at the same concentration showed sometimes the formation of amorphous aggregates.

Kinetics of unfolding intermediate formation

In the case of irreversible denaturation processes, such as those occurring by the formation of a denaturation intermediate, neither van't Hoff nor calorimetric enthalpy can be calculated. Nevertheless in such cases, the activation energy (E^{\ddagger}) for the formation of the intermediates could be deduced from the measure of the T_m at different temperature scanning rates (ν) as shown by Lumry–Eyring theory [12]. This model is restricted by two important conditions: i) the native state (N) generates only one intermediate (I) and ii) the native state and the intermediate are not in a complex equilibrium.

Assuming that these two criteria are met, DSC curves were recorded at different temperature scan rates at pH 4.0 and 7.2 for all variants. The kinetic parameters were

Table 2 Thermokinetic parameters of the formation of the unfolding intermediate (*I*) of the different sheep PrP variants at pH 4.0 and 7.2

	pH 4.0					pH 7.2						
	E^{\ddagger} kJ mol ⁻¹	ΔH^{\ddagger} kJ mol ⁻¹	ΔS^{\ddagger} kJ mol ⁻¹ K ⁻¹	ΔG^{\ddagger} kJ mol ⁻¹	ln(<i>A</i>)	k μ s ⁻¹	E^{\ddagger} kJ mol ⁻¹	ΔH^{\ddagger} kJ mol ⁻¹	ΔS^{\ddagger} kJ mol ⁻¹ K ⁻¹	ΔG^{\ddagger} kJ mol ⁻¹	ln(<i>A</i>)	k μ s ⁻¹
VRQ	564.4	561.6	1.30	111.6	184.3	26.1	681.6	678.8	1.60	131.3	218.2	0.038
ARQ	526.2	523.3	1.20	108.1	172.2	76.7	677.6	674.8	1.60	125.0	219.1	0.370
AHQ	341.8	339.0	0.65	116.0	105.3	2.9	389.7	386.8	0.77	122.3	119.7	0.373
ARR	430.5	427.6	0.91	114.0	137.0	9.3	543.8	540.6	1.20	126.1	172.0	0.158

E^{\ddagger} is the activation energy, ln(*A*) the logarithm of the transmission factor, k the first order kinetic constant determined by Arrhenius relation at 75°C, ΔH^{\ddagger} the activation enthalpy, ΔS^{\ddagger} the activation entropy change and ΔG^{\ddagger} the activation free energy at 75°C

obtained by plotting $\ln(v/T_m^2)$ as a function of $-1/RT_m$ and they are presented in Table 2. The linearity of $\ln(v/T_m^2)$ as a function of $-1/RT_m$ confirms the validity of the Lumry–Eyring treatment. At both pH 4.0 and 7.2 the formation of the unfolding intermediates requires higher activation energy in the case of VRQ and ARQ (two variants associated with the highest susceptibility) than in the case of AHQ and ARR PrP variants. The contribution of this activation energy for VRQ and ARQ in the kinetic rate constant seems to be compensated by a higher transmission factor (A). The bigger value of A means that, when variants reach the activated stage (PrP^\ddagger), the rate of unfolding intermediate formation ($\text{PrP}^\ddagger \rightarrow I$) is higher for susceptible variants.

Discussion

Prion proteins are highly stable proteins

The thermodynamic parameters measured in case of reversible denaturation (pH 4.5 and 5.0, Table 1), show for all variants unusually high values of ΔG (32.5 to 40.1 kJ mol⁻¹) and ΔH_{cal} (230 to 289 kJ mol⁻¹), considering the number of amino acids in the structured domain of the PrP protein (124–231=107 amino acids); a structured domain of about 100 amino acids should have a denaturation free energy (ΔG) of about 15 to 20 kJ mol⁻¹. This big value could be explained by the presence of a large number of salt bridges stabilizing the native state. Indeed, the difference in heat capacity (ΔC_p) between the native and the unfolded state at pH 4.5, except for VRQ, suggests low contribution of hydrophobic interactions to the stability of the protein at this pH [13]. This contribution increases at pH 5.0 (higher ΔC_p), resulting in more compact hydrophobic core, which remains in good agreement with observed ANS fluorescence changes.

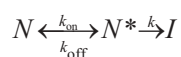
Genetic polymorphisms modulate the PrP stability

Nevertheless the measured thermodynamic parameters demonstrate marked differences depending on the sheep PrP variant. This can be explained by analysing the known bovine PrP 3D structure (31), taking into account the fact that i) the sheep ARQ variant sequence has more than 94% homology with the bovine PrP and ii) all variants can be obtained/derived from ARQ by single amino acid substitution. Two sets of PrP polymorphisms can thus be distinguished. The first one, A136V, generating the VRQ variant, leads to a stabilization (increase in ΔG^0) of the native state increasing the hydrophobic core surface area. This hypothesis is supported by the higher value of ΔC_p and ΔH_{cal} for VRQ as compared with ARQ, what reflects bigger compactness of VRQ [11]. The second set of polymorphisms, R154H and Q171R, generating AHQ and ARR, respectively, destabilizes the native state of PrP. The replacement of arginine in position 154 by histidine weakens (or makes it disappear altogether) the salt bridge with Asp 150, thus destabilizing helix 1. This leads to an exceptionally low stability of AHQ (Table 1). In the case of ARR, the suppression of a H-bond between Q171 and R167 leads to the destabilization of the junction between S2 (β -sheet 2) and H2 (helix 2).

All PrP variants give rise to heat-induced unfolding intermediates

Interestingly, at pH higher than 5.0 and lower than 4.5, curves for all variants show an irreversible thermal denaturation process and the formation of unfolding intermediates (*I*). The pH range promoting the formation of these intermediates suggests either the need of protonation acidic residues (Asp and Gln, pH<4.5) or the need for histidine deprotonation (pH>6.0). Formation of an unfolding intermediate happens already at pH 5.0 in the case of AHQ. This suggests the involvement of amino acid residue in position 154 in the formation of the intermediate. The beginning of histidine deprotonation at pH>5.0 induces the formation of the intermediate earlier than is observed in ARQ.

The existence of an equilibrium between native (*N*) and a partially unfolded native state (*N'*) prior to formation of the intermediate *I* is suggested by the presence of a well defined isodichroic point during the loss of α helix observed during the phase of the denaturation process (from 25 to 60°C). Therefore the following scheme for the unfolding process can be proposed, which may be well described by the Lumry–Eyring model (for review see [12]):



with *k* higher than *k*_{off} in the case of an irreversible denaturation. If the last condition is not met, the denaturation is a classical reversible process and the shape of curve is independent of the scan rate [12]. The Lumry–Eyring model assumes the ΔH of *N'*→*I* to be very low as compared to the ΔH of *N*↔*N'*. If not, the first peak would be deformed [13].

Refolded forms have common amyloidogenic properties

Refolding the intermediates by cooling to room temperature leads to a change of secondary structure and to the formation of amyloid fibrils. Despite differences in the secondary structure of these amyloidogenic states, no correlation between PrP polymorphisms and amyloid propensities could be observed by the technique employed, namely ThT fixation and electron microscopy. Important questions remain, however, to be answered, such as what is the effect of physico-chemical conditions on the mechanism and the rate of amyloid formation, as well as what is the possibility to produce amyloid heteropolymers between different variants linked to scrapie susceptibility (VRQ, ARQ and AHQ) and resistance (ARR). These points can be analysed in the used conditions, namely in the absence of any chemical denaturant. Particularly the protein domains involved in amyloid fibrils formation are now being studied by protease cleavage, and will be compared with the cellular degradation products.

References

- 1 S. B. Prusiner, *Science*, 216 (1982) 1309.
- 2 D. C. Bolton, M. P. McKinley and S. B. Prusiner, *Science*, 218 (1982) 1309.
- 3 N. Stahl, M. A. Baldwin and S. B. Prusiner, *Cell. Biol. Int. Rep.*, 15 (1991) 853.

- 4 W. Goldmann, N. Hunter, J. D. Foster, J. M. Salbaum, K. Beyreuther and J. Hope, *Proc. Natl. Acad. Sci. USA*, 87 (1990) 2476.
- 5 W. Goldmann, T. Martin, J. Foster, S. Hughes, G. Smith, K. Hughes, M. Dawson and N. Hunter, *J. Gen. Virol.*, 77 (1996) 2885.
- 6 P. B. Belt, I. H. Muileman, B. E. Schreuder, J. Bos-de Ruijter, A. L. Gielkens and M. A. Smits, *J. Gen. Virol.*, 76 (1995) 509.
- 7 M. A. Tranulis, A. Osland, B. Bratberg and M. J. Ulvund, *J. Gen. Virol.*, 80 (1999) 1073.
- 8 W. Swietnicki, R. B. Petersen, P. Gambetti and W. K. Surewicz, *J. Biol. Chem.*, 273 (1998) 31048.
- 9 S. Liemann and R. Glockshuber, *Biochemistry*, 38 (1999) 3258.
- 10 H. Rezaei, D. Marc, Y. Choiset, M. Takahashi, G. Hui Bon Hoa, T. Haertlé, J. Grosclaude and P. Debey, *Eur. J. Biochem.*, 267 (2000) 2833.
- 11 R. K. Meyer, A. Lustig, B. Oesch, R. Fatzer, A. Zurbriggen and M. Vandeveld, *J. Biol. Chem.*, 275 (2000) 38081.
- 12 J. M. Sanchez-Ruiz, J. L. Lopez-Lacomba, M. Cortijo and P. L. Mateo, *Biochemistry*, 27 (1988) 1648.
- 13 J. M. Sanchez-Ruiz, *Biophys. J.*, 61 (1992) 921.
- 14 P. L. Privalov, *Protein Chem.*, 33 (1979) 167.